organic compounds

(2R,4S)-7-Bromo-2-phenyl-2,3,4,5-tetrahydro-1,4-epoxynaphtho[1,2-b]-azepine, (2RS,4SR)-7-bromo-2-(4-chlorophenyl-2,3,4,5-tetrahydro-1,4-epoxynaphtho[1,2-b]azepine and (2RS,4SR)-2-(4-fluorophenyl)-2,3,4,5-tetrahydro-1,4-epoxynaphtho[1,2-b]-azepine: hydrogen-bonded structures in two and three dimensions

Alirio Palma,[a] Ali Bahsas,[b] Andrés F. Yépes,[a] Justo Cobo,[c] Michael B. Hursthouse[d] and Christopher Glidewell[e]*

[a]Laboratorio de Síntesis Orgánica, Escuela de Química, Universidad Industrial de Santander, AA 678 Bucaramanga, Colombia, [b]Laboratorio de RMN, Grupo de Productos Naturales, Departamento de Química, Universidad de los Andes, Mérida 5101, Venezuela, [c]Departamento de Química Inorgánica y Orgánica, Universidad de Jaén, 23071 Jaén, Spain, [d]School of Chemistry, University of Southampton, Highfield, Southampton SO17 1BJ, England, and [e]School of Chemistry, University of St Andrews, Fife KY16 9ST, Scotland

Correspondence e-mail: cg@st-andrews.ac.uk

(2R,4S)-7-Bromo-2-phenyl-2,3,4,5-tetrahydro-1,4-epoxynaphtho-[1,2-b]azepine, $C_{20}H_{16}BrNO$, (I), exhibits evidence of a modest degree (ca 10%) of inversion twinning, while both (2RS,4SR)-7-bromo-2-(4-chlorophenyl)-2,3,4,5-tetrahydro-1,4-epoxynaphtho[1,2-b]azepine, $C_{20}H_{15}BrClNO$, (II), and (2RS,-4SR)-2-(4-fluorophenyl)-2,3,4,5-tetrahydro-1,4-epoxynaphtho-[1,2-b]azepine, $C_{20}H_{16}FNO$, (III), crystallize as genuine racemic mixtures. The molecules of (I) are linked into sheets by a combination of one C—H···O hydrogen bond and two C—H···π(arene) hydrogen bonds, while those of (II) are linked into sheets of π-stacked hydrogen-bonded chains. A combination of one C—H···O hydrogen bond and four independent C—H···π(arene) hydrogen bonds links the molecules of (III) into a three-dimensional framework. The significance of this study lies in its finding, via comparison with the structures of some closely-related epoxybenzazepine analogues, of significant changes in crystal structures consequent upon small changes in the peripheral substituents.

Comment

As part of a wider programme aimed at the synthesis and characterization of novel fused azepines as potential anti-protozoal agents (Gómez et al., 2006; Yépez et al., 2006), we have recently reported on the molecular structures and supramolecular aggregation in several different types of substituted tetrahydro-1,4-epoxy-1-benzazepines (Acosta et al., 2008; Blanco et al., 2008; Gómez et al., 2008). We have now extended this study to encompass analogues containing the tetrahydro-1,4-epoxynaphtho[2,1-b]azepine framework, and report here the structures of three such compounds, namely (2R,4S)-7-bromo-2-exo-4-phenyl-2,3,4,5-tetrahydro-1H-1,4-epoxynaphtho[2,1-b]azepine, (I), (2RS,4SR)-7-bromo-2-exo-4-(4-chlorophenyl-2,3,4,5-tetrahydro-1H-1,4-epoxynaph-tho[2,1-b]azepine, (II), and (2RS,4SR)-2-exo-4-(4-fluorophen-yl)-2,3,4,5-tetrahydro-1H-1,4-epoxynaphtho[2,1-b]azepine, (III) (Figs. 1–3).
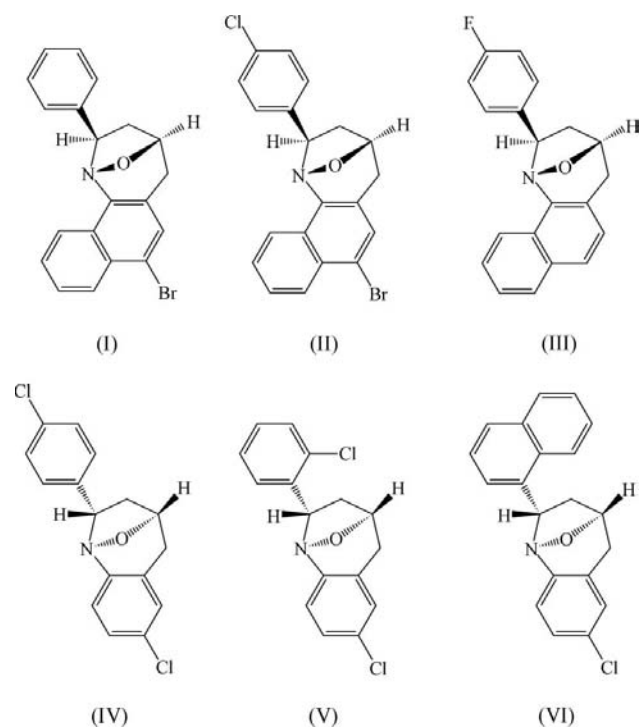
While (II) and (III) crystallize as racemic mixtures in the space groups Pbca and $P2_1/c$, respectively, (I) crystallizes in the space group $P2_1$ and was handled as an inversion twin, giving twin fractions for the crystal selected for data collection of 0.901 (15) for the 2R,4S enantiomer and 0.099 (15) for the 2S,4R enantiomer. Accordingly, the reference molecule in racemic compounds (II) and (III) were each selected as having the 2R,4S configuration. This behaviour in (I)–(III) may be contrasted with the behaviour (Gómez et al., 2008) of the aryl-substituted tetrahydro-1,4-epoxy-1-benzazepines (IV)–(VI) (see scheme). Compound (IV) crystallizes as a racemic mixture in the space group $Pna2_1$, while each of (V) and (VI) crystallizes as a single enantiomorph, both in the space group $P2_12_12_1$, having the opposite configuration (viz. 2S,4R), as shown by the values of the Flack (1983) x parameter. Since the majority of the other substituted tetrahydro-1,4-epoxy-1-benzazepines that we have studied recently have been found to crystallize either as true racemic mixtures (Blanco et al.,

2008) or as inversion twins containing unequal numbers of the two enantiomers (Acosta *et al.*, 2008), it seems likely that all such species are, in fact, synthesized as racemic mixtures, particularly since their syntheses offer no obvious scope for enantiospecific discrimination. It is surprising, however, that of the 12 fused epoxyazepines of this type studied to date by
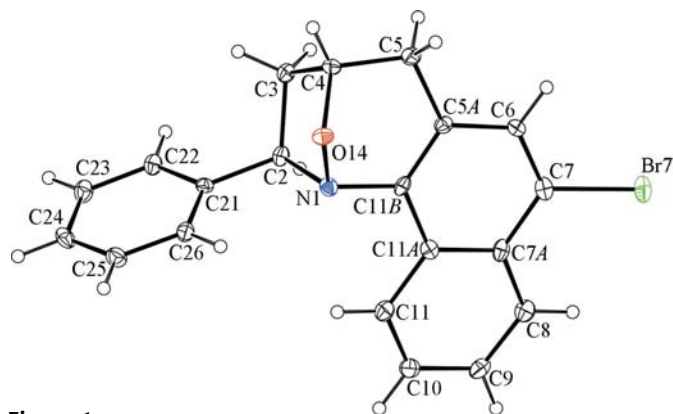

Figure 1
The molecular structure of (I), with configuration 2*R*,4*S*, showing the atom-labelling scheme. Displacement ellipsoids are drawn at the 30% probability level.
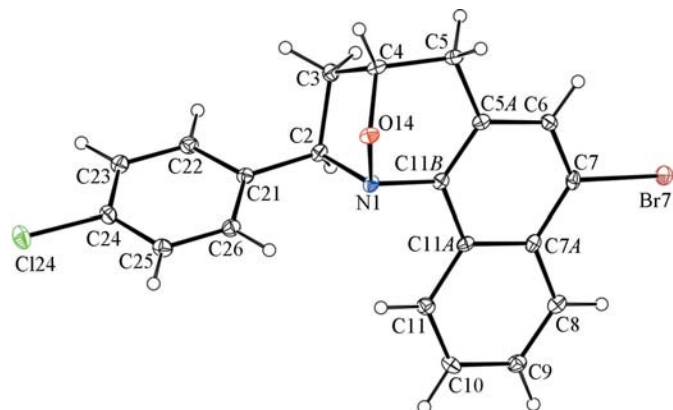

Figure 2
The molecular structure of the 2*R*,4*S* enantiomer in racemic compound (II), showing the atom-labelling scheme. Displacement ellipsoids are drawn at the 30% probability level.

Figure 3
The molecular structure of the 2*R*,4*S* enantiomer in racemic compound (III), showing the atom-labelling scheme. Displacement ellipsoids are drawn at the 30% probability level.
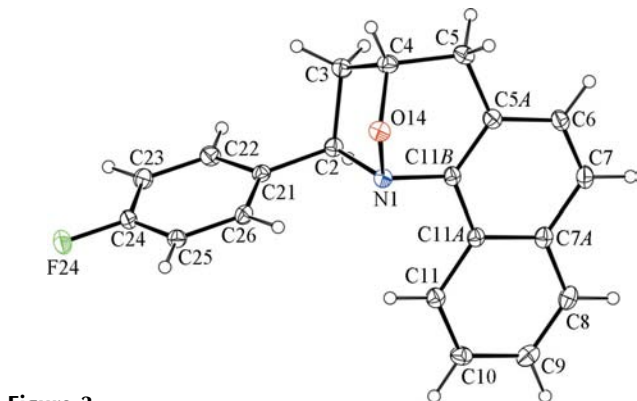
us, including the three reported here, only six crystallize in space groups containing reflection or inversion operators; the other six all crystallize either in $P2_1$ or in $P2_12_12_1$, three as inversion twins and only three as single enantiomers.

The conformations of the fused heterocyclic systems in (I)–(III) are extremely similar, as shown by the values (Table 1) of the ring-puckering parameters (Cremer & Pople, 1975). The five-membered ring components adopt envelope conformations, folded across the N1···C4 line (Figs. 1–3), while the six-membered rings have conformations intermediate between envelope and half-chair forms, where the idealized values of the ring-puckering angles are $\theta = 54.7°$ and $\varphi = 60n°$, and $\theta = 50.8°$ and $\varphi = (60n + 30)°$, respectively (n represents an integer). The N1—C2—C21—C22 torsion angles describing the orientation of the pendent aryl ring relative to the azepine ring are also fairly similar: $-177.3 (4)°$ in (I), 172.4 (3)° in (II) and $-171.98 (17)°$ in (III).

Despite the rather similar conformations, and the overall similarity in the molecular shapes in (I)–(III), the patterns of their supramolecular aggregation are significantly different. The hydrogen-bonded structure of (I) is dominated by one C—H···O hydrogen bond and two C—H···π(arene) hydrogen bonds (Table 2). There is a short C—H···Br contact in this structure, but this involves an aliphatic C—H bond of fairly low acidity and, more importantly, it has been shown that Br bonded to C is an extremely poor acceptor of hydrogen bonds (Aakeröy *et al.*, 1999; Brammer *et al.*, 2001; Thallapally & Nangia, 2001); accordingly, this contact must be regarded as being not structurally significant. The C—H···O hydrogen bond links molecules related by the 2_1 screw axis along (0, *y*, 1) into a $C(7)$ (Bernstein *et al.*, 1995) chain running parallel to the [010] direction. At the same time, the C—H···π(arene) hydrogen bond having aryl atom C23 as the donor links molecules related by translation along [010]. The combination of these two interactions then generates a chain of rings running parallel to the [010] direction (Fig. 4). The other C—H···π(arene) hydrogen bond has an aliphatic C atom as the donor and the pendent phenyl ring as the
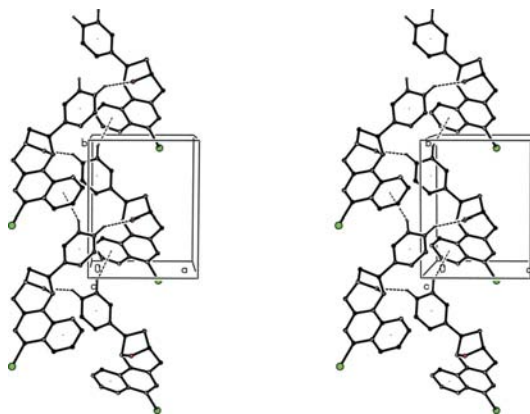

Figure 4
A stereoview of part of the crystal structure of (I), showing the formation of a chain of rings along (0, *y*, 1) formed by the two hydrogen bonds having aryl C atoms as the donors. For the sake of clarity, H atoms not involved in the motifs shown have been omitted.

acceptor, and its effect is to link molecules related by the 2_1 screw axis along $(\frac{1}{2}, y, 1)$ into a second chain running parallel to the [010] direction (Fig. 5). The combined action of the two independent [010] chains is to link the molecules into a sheet parallel to (001). There are no direction-specific interactions between adjacent sheets, so that the hydrogen-bonded structure in (I) is two-dimensional.

Molecules of (II) related by the *b*-glide plane at $x = \frac{1}{4}$ are linked by a single rather weak C—H···O hydrogen bond (Table 2) into a $C(4)$ chain running parallel to the [010] direction. Chains of this type are linked into sheets by a single aromatic π–π stacking interaction. The chlorinated aryl rings of the molecules at (x, y, z) and $(-x + 1, -y + 1, -z + 1)$ are strictly parallel, with an interplanar spacing of 3.500 (2) Å. The ring-centroid separation is 3.833 (2) Å, corresponding to a ring-centroid offset of 1.563 (2) Å. The effect of this interaction is to link the $C(4)$ chain involving the glide plane at $x = \frac{1}{4}$

to the two chains involving glide planes at $x = \frac{3}{4}$ and $x = -\frac{1}{4}$, so generating a sheet of π-stacked hydrogen-bonded chains lying parallel to (001) (Fig. 6).

The hydrogen-bonded structure of (III) is three-dimensional and is determined by a combination of one C—H···O hydrogen bond and four independent C—H···π(arene) hydrogen bonds; in the event, just three of these interactions suffice to demonstrate the three-dimensional nature of the hydrogen-bonded structure. The C—H···π(arene) interaction having atom C3 as the donor links molecules related by the *c*-glide plane at $y = \frac{3}{4}$ into a chain running parallel to the [001] direction (Fig. 7), while that having atom C5 as the donor links molecules related by the 2_1 screw axis along $(\frac{1}{2}, y, \frac{1}{4})$ into a chain running parallel to the [010] direction (Fig. 8). The combination of these two chains generates a sheet parallel to (100), and a third hydrogen bond links adjacent sheets to form a continuous three-dimensional framework *via* a cyclic centrosymmetric motif (Fig. 9). The C—H···O hydrogen bond lies within the (100) sheet, while the final C—H···π(arene) interaction reinforces, albeit weakly, the linking of adjacent (100) sheets.

It is of interest briefly to compare the hydrogen-bonded structures of compounds (I)–(III) with those of the benzaze-
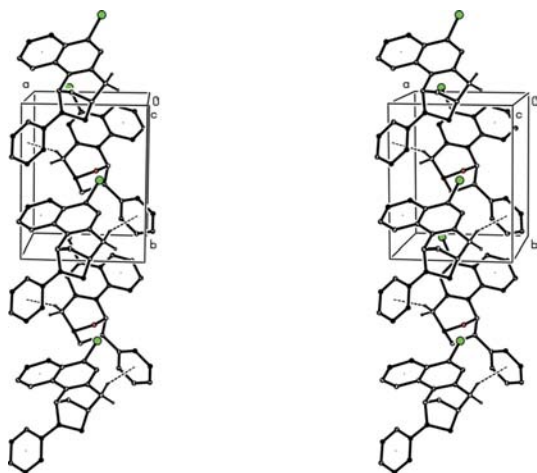

Figure 5
A stereoview of part of the crystal structure of (I), showing the formation of a chain along $(\frac{1}{2}, y, 1)$ formed by the single hydrogen bond having an aliphatic C atom as the donor. For the sake of clarity, H atoms not involved in the motif shown have been omitted.
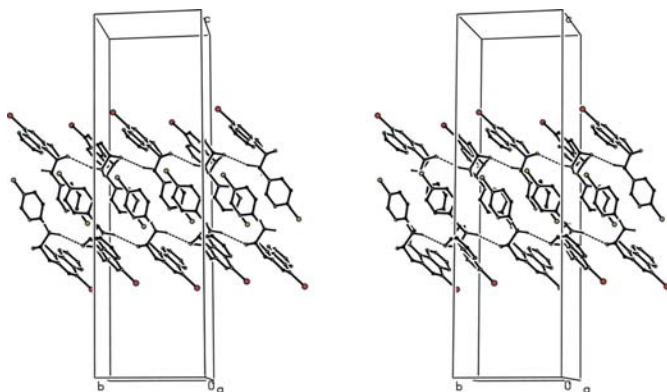

Figure 7
A stereoview of part of the crystal structure of (III), showing the formation of a chain running parallel to [001]. For the sake of clarity, H atoms not involved in the motif shown have been omitted.

Figure 6
A stereoview of part of the crystal structure of (II), showing two of the $C(4)$ hydrogen-bonded chains, those based on the glide planes at $x = \frac{1}{4}$ and $x = \frac{3}{4}$, which form part of the (001) sheet of π-stacked chains. For the sake of clarity, H atoms not involved in the motif shown have been omitted.
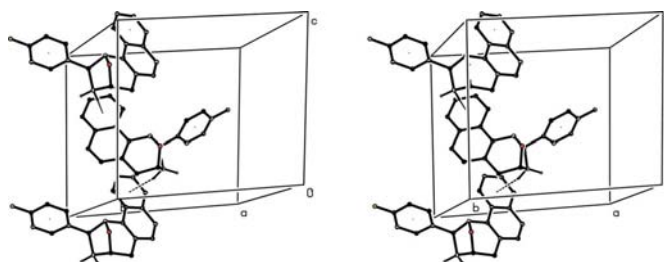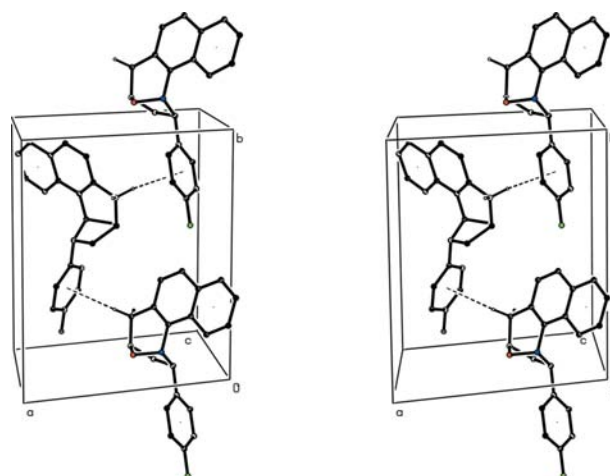

Figure 8
A stereoview of part of the crystal structure of (III), showing the formation of a chain running parallel to [010]. For the sake of clarity, H atoms not involved in the motif shown have been omitted.
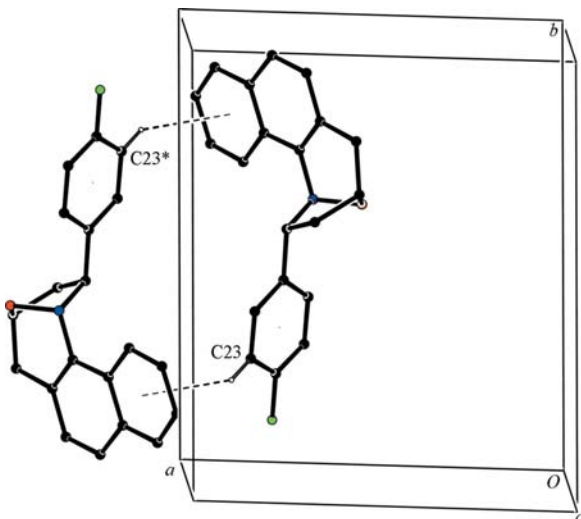
organic compounds

Figure 9
Part of the crystal structure of (III), showing the formation of a cyclic centrosymmetric motif which links adjacent (100) sheets. For the sake of clarity, H atoms not involved in the motif shown have been omitted. The atom marked with an asterisk (*) is at the symmetry position $(-x + 2, -y + 1, -z + 1)$.

pine analogues (IV)–(VI) (Gómez *et al.*, 2008). In mono-halogenated compound (VI), a combination of one C—H⋯O hydrogen bond and two C—H⋯π(arene) hydrogen bonds generates a three-dimensional structure in the space group $P2_12_12_1$. Two substructures can readily be identified, one of them one-dimensional and the other two-dimensional. Not only do the two isomeric dichloro compounds (IV) and (V) exhibit different space groups ($Pna2_1$ and $P2_12_12_1$, respectively) with very different unit-cell dimensions, but their hydrogen-bonded structures also differ considerably. In (IV), a combination of C—H⋯O and C—H⋯N hydrogen bonds generates a chain of edge-fused $R_3^3(12)$ rings; this is the only example so far studied whose structure both contains a C—H⋯N hydrogen bond and does not contain a C—H⋯π(arene) hydrogen bond. In the structure of (IV), one C—H⋯O and two C—H⋯π(arene) hydrogen bonds acting individually generate three orthogonal chains of molecules related by different 2_1 screw axes which, in combination, give rise to a three-dimensional framework structure. Thus, although the hydrogen-bonded structures in (III), (V) and (VI) are all three-dimensional, there are few if any similarities in the detailed construction of the frameworks involved. The differences in crystal structures observed for (I)–(VI) are all consequent upon rather modest changes in the substituents.

Experimental

To a stirred solution of 0.10 mol of the appropriately substituted 2-allyl-*N*-benzyl-1-naphthylamine in methanol (40 ml) was added sodium tungstate dihydrate, $Na_2WO_4\cdot2H_2O$ (5 mol%), followed by 30% aqueous hydrogen peroxide solution (0.30 mol). The resulting mixtures were then stirred at room temperature for 45–50 h. Each mixture was filtered and then evaporated to dryness. The crude products were purified by column chromatography on silica gel using

heptane/ethyl acetate (30:1 *v*/*v*) as eluant. Finally, the resulting 2-*exo*-aryl-1,4-epoxy cycloadducts were recrystallized from heptane, providing crystals of compounds (I)–(III) suitable for single-crystal X-ray diffraction. For (I), colourless crystals, yield 52%, m.p. 412–413 K; MS (70 eV) m/z (%): 365 (M^+, ^{79}Br, 10), 336 (5), 286 (2), 257 (9), 243 (22), 220 (100), 180 (4), 139 (28), 128 (14), 115 (6); analysis found: C 65.7, H 4.4, N 3.8%; $C_{20}H_{16}BrNO$ requires: C 65.6, H 4.4, N 3.8%. For (II), colourless crystals, yield 48%, m.p. 459–460 K; MS (70 eV) m/z (%): 399 (M^+, ^{79}Br, ^{35}Cl, 5), 370 (3), 291 (6), 277 (14), 220 (100), 180 (5), 152 (5), 139 (33), 128 (19), 115 (5); analysis found: C 59.9, H 3.8, N 3.6%; $C_{20}H_{15}BrClNO$ requires: C 59.95, H 3.8, N 3.5%. For (III), pale-yellow crystals, yield 49%, m.p. 401–402 K; MS (70 eV) m/z (%): 305 (M^+, 10), 276 (5), 262 (14), 142 (100), 115 (17); analysis found: C 78.5, H 5.3, N 4.6%; $C_{20}H_{16}FNO$ requires: C 78.7, H 5.3, N 4.6%.

Compound (I)

Crystal data

$C_{20}H_{16}BrNO$	$V = 776.08$ (5) Å^3
$M_r = 366.24$	$Z = 2$
Monoclinic, $P2_1$	Mo $K\alpha$ radiation
$a = 7.8444$ (3) Å	$\mu = 2.65$ mm^{-1}
$b = 9.8146$ (4) Å	$T = 120$ K
$c = 10.0871$ (4) Å	$0.20 \times 0.04 \times 0.01$ mm
$\beta = 92.103$ (3)°	

Data collection

Bruker–Nonius KappaCCD diffractometer	7511 measured reflections
Absorption correction: multi-scan (*SADABS*; Sheldrick, 2003)	3132 independent reflections
$T_{min} = 0.619$, $T_{max} = 0.974$	2810 reflections with $I > 2\sigma(I)$
	$R_{int} = 0.055$

Refinement

$R[F^2 > 2\sigma(F^2)] = 0.046$	H-atom parameters constrained
$wR(F^2) = 0.102$	$\Delta\rho_{max} = 0.44$ e Å^{-3}
$S = 1.09$	$\Delta\rho_{min} = -0.53$ e Å^{-3}
3132 reflections	Absolute structure: Flack (1983), 1237 Friedel pairs
209 parameters	Flack parameter: 0.099 (15)
1 restraint	

Compound (II)

Crystal data

$C_{20}H_{15}BrClNO$	$V = 3185.0$ (7) Å^3
$M_r = 400.69$	$Z = 8$
Orthorhombic, $Pbca$	Mo $K\alpha$ radiation
$a = 9.7758$ (16) Å	$\mu = 2.76$ mm^{-1}
$b = 9.8211$ (14) Å	$T = 120$ K
$c = 33.174$ (3) Å	$0.32 \times 0.12 \times 0.04$ mm

Data collection

Bruker–Nonius KappaCCD diffractometer	28541 measured reflections
Absorption correction: multi-scan (*SADABS*; Sheldrick, 2003)	3658 independent reflections
$T_{min} = 0.551$, $T_{max} = 0.896$	2574 reflections with $I > 2\sigma(I)$
	$R_{int} = 0.073$

Refinement

$R[F^2 > 2\sigma(F^2)] = 0.042$	217 parameters
$wR(F^2) = 0.088$	H-atom parameters constrained
$S = 1.06$	$\Delta\rho_{max} = 0.39$ e Å^{-3}
3658 reflections	$\Delta\rho_{min} = -0.51$ e Å^{-3}

organic compounds

Compound (III)

Crystal data

$C_{20}H_{16}FNO$
$M_r = 305.34$
Monoclinic, $P2_1/c$
$a = 11.3036 (4)$ Å
$b = 12.7585 (5)$ Å
$c = 11.1730 (3)$ Å
$\beta = 109.137 (2)°$

$V = 1522.29 (9)$ Å^3
$Z = 4$
Mo $K\alpha$ radiation
$\mu = 0.09$ mm^{-1}
$T = 120$ K
$0.09 \times 0.08 \times 0.03$ mm

Data collection

Bruker–Nonius KappaCCD diffractometer
Absorption correction: multi-scan (*SADABS*; Sheldrick, 2003)
$T_{min} = 0.986$, $T_{max} = 0.997$

15443 measured reflections
3467 independent reflections
2667 reflections with $I > 2\sigma(I)$
$R_{int} = 0.044$

Refinement

$R[F^2 > 2\sigma(F^2)] = 0.061$
$wR(F^2) = 0.123$
$S = 1.11$
3467 reflections

208 parameters
H-atom parameters constrained
$\Delta\rho_{max} = 0.26$ e Å^{-3}
$\Delta\rho_{min} = -0.24$ e Å^{-3}

Table 1
Ring-puckering parameters (Å, °) for compounds (I)–(III).

Puckering parameters for five-membered rings are defined for the atom sequence O14—N1—C2—C3—C4, puckering parameters for six-membered rings are defined for the atom sequence O14—N1—C11B—C5A—C5—C4 and puckering parameters for seven-membered rings are defined for the atom sequence N1—C2—C3—C4—C5—C5A—C11B.

Parameter	(I)	(II)	(III)
Five-membered rings			
Q_2	0.430 (5)	0.442 (3)	0.449 (2)
φ_2	7.9 (7)	16.2 (4)	10.7 (3)
Six-membered rings			
Q	0.628 (5)	0.617 (3)	0.6223 (19)
θ	124.4 (5)	128.3 (3)	126.51 (18)
φ	170.1 (5)	165.1 (4)	166.1 (2)
Seven-membered rings			
Q	1.077 (5)	1.101 (3)	1.085 (2)
φ_2	18.7 (3)	15.80 (17)	17.09 (12)
φ_3	302.2 (8))	298.8 (6)	302.6 (4)

Table 2
Parameters (Å, °) for hydrogen bonds and short intermolecular contacts in (I)–(III).

$Cg1$ represents the centroid of the C21–C26 ring and $Cg2$ represents the centroid of the C7A/C8–C11/C11A ring.

Compound	$D—H\cdots A$	$D—H$	$H\cdots A$	$D\cdots A$	$D—H\cdots A$
(I)	C2—H2$\cdots$Br7^i	1.00	2.90	3.891 (5)	171
	C5—H52$\cdots$Cg1^{ii}	0.99	2.55	3.484 (5)	157
	C23—H23$\cdots$Cg2^{iii}	0.95	2.70	3.596 (5)	157
	C24—H24$\cdots$O14^{iv}	0.95	2.53	3.313 (6)	140
(II)	C3—H31$\cdots$O14^v	0.99	2.52	3.485 (4)	164
(III)	C3—H31$\cdots$Cg2^{vi}	0.99	2.63	3.575 (2)	160
	C5—H52$\cdots$Cg1^{vii}	0.99	2.72	3.605 (2)	149
	C9—H9$\cdots$Cg1^{viii}	0.95	2.92	3.684 (2)	139
	C23—H23$\cdots$Cg2^{ix}	0.95	2.85	3.683 (3)	147
	C25—H25$\cdots$O14^x	0.95	2.55	3.184 (3)	125

Symmetry codes: (i) $-x+1, y+\frac{1}{2}, -z+1$; (ii) $-x+1, y-\frac{1}{2}, -z+2$; (iii) $x, y+1, z$; (iv) $-x, y+\frac{1}{2}, -z+2$; (v) $-x+\frac{1}{2}, y-\frac{1}{2}, z$; (vi) $x, -y+\frac{3}{2}, z-\frac{1}{2}$; (vii) $-x+1, y+\frac{1}{2}, -z+\frac{1}{2}$; (viii) $-x+2, y+\frac{1}{2}, -z+\frac{3}{2}$; (ix) $-x+2, -y+1, -z+1$; (x) $-x+1, -y+1, -z+1$.

For (I), the systematic absences permitted $P2_1$ and $P2_1/m$ as possible space groups; $P2_1$ was selected and confirmed by the successful structure analysis. For (II) and (III), the space groups were uniquely assigned from the systematic absences. All H atoms were located in difference maps and then treated as riding atoms in geometrically idealized positions, with C—H distances of 0.95 (aromatic), 0.99 (CH$_2$) or 1.00 Å (aliphatic C—H) and with U_{iso}(H) values set at $1.2U_{eq}$(C). A straightforward ('hole-in-one') calculation of the Flack (1983) x parameter for (I) gave a value of 0.089 (14), with a Hooft y parameter (Hooft *et al.*, 2008) of 0.186 (12). In the presence of a Br atom, the deviation from zero of the Flack x parameter was significant and it seemed rather large, possibly suggesting a modest degree of inversion twinning. Calculation of the twin fractions using the TWIN/BASF procedure in *SHELXL* (Sheldrick, 2008) gave, for the crystal under study, a twin fraction of 0.901 (15) for the 2*R*,4*S* enantiomer and 0.099 (15) for the 2*S*,4*R* form. Accordingly, the 2*R*,4*S* configuration was selected for the reference molecules in the racemic compounds (II) and (III).

For all compounds, data collection: *COLLECT* (Hooft, 1999); cell refinement: *DIRAX/LSQ* (Duisenberg *et al.*, 2000); data reduction: *EVALCCD* (Duisenberg *et al.*, 2003); program(s) used to solve structure: *SIR2004* (Burla *et al.*, 2005); program(s) used to refine structure: *OSCAIL* (McArdle, 2003) and *SHELXL97* (Sheldrick, 2008); molecular graphics: *PLATON* (Spek, 2009); software used to prepare material for publication: *SHELXL97* and *PRPKAPPA* (Ferguson, 1999).

Supplementary data for this paper are available from the IUCr electronic archives (Reference: SK3295). Services for accessing these data are described at the back of the journal.

References

Aakeröy, C. B., Evans, T. A., Seddon, K. R. & Pálinkó, I. (1999). *New J. Chem.* pp. 145–152.
Acosta, L. M., Bahsas, A., Palma, A., Cobo, J., Low, J. N. & Glidewell, C. (2008). *Acta Cryst.* C**64**, o514–o518.
Bernstein, J., Davis, R. E., Shimoni, L. & Chang, N.-L. (1995). *Angew. Chem. Int. Ed. Engl.* **34**, 1555–1573.
Blanco, M. C., Raysth, W., Palma, A., Cobo, J., Low, J. N. & Glidewell, C. (2008). *Acta Cryst.* C**64**, o524–o528.
Brammer, L., Bruton, E. A. & Sherwood, P. (2001). *Cryst. Growth Des.* **1**, 277–290.
Burla, M. C., Caliandro, R., Camalli, M., Carrozzini, B., Cascarano, G. L., De Caro, L., Giacovazzo, C., Polidori, G. & Spagna, R. (2005). *J. Appl. Cryst.* **38**, 381–388.
Cremer, D. & Pople, J. A. (1975). *J. Am. Chem. Soc.* **97**, 1354–1358.
Duisenberg, A. J. M., Hooft, R. W. W., Schreurs, A. M. M. & Kroon, J. (2000). *J. Appl. Cryst.* **33**, 893–898.
Duisenberg, A. J. M., Kroon-Batenburg, L. M. J. & Schreurs, A. M. M. (2003). *J. Appl. Cryst.* **36**, 220–229.
Ferguson, G. (1999). *PRPKAPPA*. University of Guelph, Canada.
Flack, H. D. (1983). *Acta Cryst.* A**39**, 876–881.
Gómez, S. L., Raysth, W., Palma, A., Cobo, J., Low, J. N. & Glidewell, C. (2008). *Acta Cryst.* C**64**, o519–o523.

Gómez, S. L., Stashenko, E., Palma, A., Bahsas, A. & Amaro-Luis, J. M. (2006). *Synlett*, pp. 2275–2277.

Hooft, R. W. W. (1999). *COLLECT*. Nonius BV, Delft, The Netherlands.

Hooft, R. W. W., Straver, L. H. & Spek, A. L. (2008). *J. Appl. Cryst.* **41**, 96–103.

McArdle, P. (2003). *OSCAIL for Windows*. Version 10. Crystallography Centre, Chemistry Department, NUI Galway, Ireland.

Sheldrick, G. M. (2003). *SADABS*. Version 2.10. University of Göttingen, Germany.

Sheldrick, G. M. (2008). *Acta Cryst.* A**64**, 112–122.

Spek, A. L. (2009). *Acta Cryst.* D**65**, 148–155.

Thallapally, P. K. & Nangia, A. (2001). *CrystEngComm*, **27**, 1–6.

Yépez, A. F., Palma, A., Stashenko, E., Bahsas, A. & Amaro-Luis, J. (2006). *Tetrahedron Lett.* **47**, 5825–5828.